PHYSICAL REVIEW A VOLUME 39, NUMBER 2 JANUARY 15, 1989

Complementarity in a quantum nondemolition measurement

B. C. Sanders and G. J. Milburn
Department of Physics, University of Queensland, St. Lucia, Queensland 4067, Australia
(Received 13 July 1988; revised manuscript received 9 September 1988)

We present an analysis of a quantum nondemolition (QND) measurement, which determines which of the two possible paths a photon follows through a Mach-Zehnder interferometer. The measurement is effected by the nonlinear Kerr effect. If a photon traverses the arm of the interferometer containing the Kerr medium, it shifts the phase of a probe beam and then continues through to the interferometer output. The measurement does not destroy the photon but does disturb its phase. Using various probe states, we show how such phase disturbances reduce fringe visibility and enforce a principle of complementarity; the more accurately the QND measurement determines the path of the photon, the lower is the fringe visibility. We determine the appropriate parameters to optimize the observation of the two complementary quantities.

I. INTRODUCTION

Photons, like all quantum objects exhibit corpuscular or wavelike behavior under different experimental conditions. It is not possible to consistently attribute corpuscular properties and wavelike properties to a photon. Rather we say that corpuscular or wavelike behavior is a complementary aspect of the photon. Here we concern ourselves with a model experiment which reveals a continuous transition from wavelike to corpuscular behavior of the photon by adjusting one parameter in the apparatus.

The corpuscular behavior is revealed by placing a beamsplitter in the path of a one-photon state. A photon detector placed at the output port detects either one or zero photons. The photon exhibits corpuscular behavior by remaining whole, whereas a wave would be split by the beamsplitter. If instead the photon passes through an interferometer, a different result is observed. The photon passes through a beamsplitter. The photon is presented with two paths to follow and then is recombined by a beamsplitter, and a measurement is performed by a photon detector. A phase shifter is inserted to allow for a variation of the path difference between the two arms. An ensemble of single-photon interference experiments for varying values of the path difference demonstrates the existence of interference fringes. The single photon is exhibiting wavelike behavior by apparently following both paths and interfering with itself.

The two experiments described above have been performed[1] and have demonstrated the corpuscular and wavelike behavior under the appropriate experimental conditions. The first experiment detected a strong anticorrelation between photon arrivals at the two photon detectors when a single photon encountered a beamsplitter. The second experiment required a sequence of single-photon interference measurements in a Mach-Zehnder interferometer for each value of the phase as determined by the phase shifter, and the accumulated result demonstrated the effect of single-photon interference. However, Grangier *et al.* do suggest that a quantum nondemolition (QND) device could be employed, which would allow the simultaneous measurement of the interference at the interferometer output and the presence of the photon in one arm of the interferometer.

Here we design an experiment which employs a photon number QND measurement[2,3] in one interferometer arm. The QND measurement is employed in order to determine the presence of a photon without destroying the photon, in contrast to the destructive nature of the photon detector. We shall see how the certainty of measuring a photon along one arm of the interferometer affects the observation of interference fringes at the interferometer output, and therefore observe the effect of measurement on the wavelike behavior quantitatively.

An experiment which involves a refractive medium in one of the interferometer arms which absorbs some of the momentum of the photon has been discussed.[4] A measurement of the momentum transferred to the medium provides information about the path the photon went along and simultaneously destroys the interference fringes due to the momentum uncertainty. However, the apparatus that we present allows for a complete analysis of the quantum state of the measurement device in the interferometer and its preparation. Also the scheme presented here is closer to experimental realization.

II. PHOTON NUMBER QND MEASUREMENT AND THE OPTICAL KERR EFFECT

For a QND determination of the photon path, it is necessary to place a detector along one arm which will provide information about the photon number but which will leave the number operator in the Heisenberg picture unchanged by the interaction with the detector. Detection causes a back action, but the back action in this case must be confined to affecting the phase of the field. For the number operator to be a QND variable we require that it be isolated from such phase disturbances. This is automatically satisfied if the number operator is a constant of motion in the absence of the measurement. Such a QND measurement could be made using the optical Kerr effect which we briefly describe.

In the optical Kerr effect two single-mode fields are

sent through a nonlinear crystal. The annihilation operator for the probe field is B and a_2 is the annihilation operator for the field through arm 2 of the interferometer. The Hamiltonian for the system is given by

$$H=\hbar\omega_a n_2+\hbar\omega_B n_B+2\hbar\chi n_2 n_B+\tfrac{1}{2}\hbar\chi_a n_2^2+\tfrac{1}{2}\hbar\chi_B n_B^2 , \tag{2.1}$$

where the number operators are defined by

$$n_B=B^\dagger B \text{ and } n_i=a_i^\dagger a_i, \quad i=1 \text{ or } 2 , \tag{2.2}$$

and the angular frequencies for the modes are ω_a and ω_B. The parameters of nonlinearity are χ, χ_a, and χ_B, which are frequency dependent. The parameters are elements of the $\chi^{(3)}$ tensor for the particular medium. Experiments to measure the observables corresponding to the Hamiltonian have been analyzed[5] and performed[6] in optical fibers in a cavity for which the values of χ, χ_a, and χ_B are equal. At the other extreme are the analyses in which χ_a and χ_B are both zero.[2,3]

The Heisenberg equations of motion for the operators are

$$da_2/dt=-i(\omega_a'+2\chi n_B+\chi_a n_2)a_2 \tag{2.3a}$$

and

$$dB/dt=-i(\omega_B'+2\chi n_2+\chi_B n_B)B , \tag{2.3b}$$

where

$$\omega_{a,B}'=\omega_{a,B}+\chi_{a,B} . \tag{2.4}$$

As the number operators n_2 and n_B are constants of motion, the operators after the interaction are given by

$$a_2'=\exp[-i(\varphi+\omega_a'+2\chi n_B+\chi_a n_2)]a_2 , \tag{2.5a}$$

where φ is the phase of the phase shifter and

$$B'=\exp[-i(\omega_B'+2\chi n_2+\chi_B n_B)]B , \tag{2.5b}$$

where the interaction time in the crystal is set as unity. The number operators after the interaction are

$$n_2'=n_2 \text{ and } n_B'=n_B . \tag{2.6}$$

Therefore, the interaction has altered the phase of the fields but not the photon number. Thus, the insertion of the Kerr medium along one arm of the interferometer will not affect the photon number distribution along that arm.

III. INTERFEROMETER OUTPUT FRINGES

The inclusion of the photon number QND measurement device in the interferometer is depicted in Fig. 1. The probe field undergoes a quadrature phase measurement (QPM) which will be discussed further in Sec. V. As the nonlinear Kerr medium causes the fields a_2 and B to induce phase changes in each other, a phase-sensitive measurement of the probe field is necessary to determine the nature of the field a_2.

The interferometer output field b is a superposition of the fields a_1 and a_2' given by

$$b=2^{-1/2}(a_1+ia_2') . \tag{3.1}$$

The photon detector measures the photon number and the number operator is

$$n_b=b^\dagger b=\tfrac{1}{2}(n_1+n_2)+\frac{1}{2i}(a_2'^\dagger a_1-a_2'a_1^\dagger) . \tag{3.2}$$

We are interested in the case that one photon is injected into the interferometer. In this case the field inside the interferometer is given by

$$|\Psi\rangle=2^{-1/2}(|1\rangle_1\otimes|0\rangle_2-i|0\rangle_1\otimes|1\rangle_2) \tag{3.3}$$

which represents the superposition of the photon in one arm and the vacuum in the second arm with the case of the vacuum in the first arm and the photon in the second arm and is consistent with the beamsplitter transformation (3.1). The $\frac{50}{50}$ beamsplitter does not change the phase of the transmitted field, but the reflected state undergoes a phase change of $\pi/2$; the phase of the terms in the sum (3.3) is a consequence of these induced phased shifts. Given that the density matrix for the probe is ρ_B, we define a function $Z(\chi)$ by

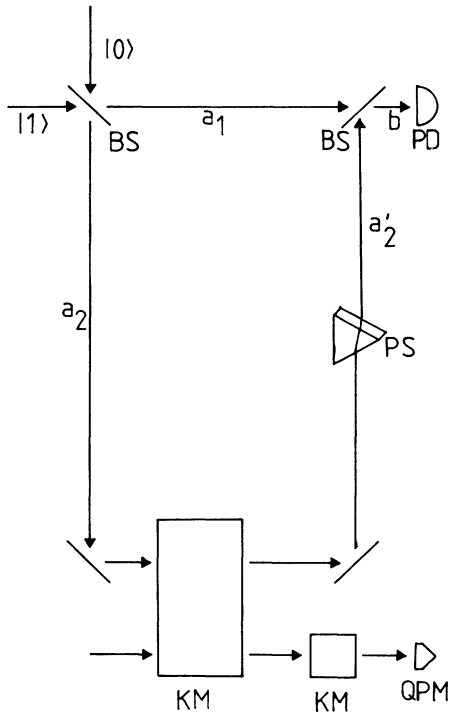

FIG. 1. Quantum nondemolition measurement of complementarity. A one-photon state $|1\rangle$ and the vacuum $|0\rangle$ are injected into a Mach-Zehnder interferometer with $\frac{50}{50}$ beamsplitters (BS). The interferometer output photons are detected by the photon detector (PD). The phase shifter (PS) allows for adjustments of the phase difference between the two paths. A Kerr medium (KM) is placed in arm 2 of the interferometer. The probe field (B) interacts with the field in arm 2 of the interferometer via the KM, encounters a second KM, and is detected by a quadrature phase measurement apparatus (QPM).

$$Z(\chi)\equiv \mathrm{tr}_B[\rho_B \exp(2i\chi n_B)]$$
$$= \sum_{n=0}^{\infty} P_B(n) e^{2i\chi n} , \tag{3.4}$$

where $P_B(n)$ is the photon number distribution in the probe state. The mean photon number measured by the photon detector is

$$\langle n_b \rangle = \tfrac{1}{2} + \mathrm{Re}[\exp(i\Omega_a) Z(\chi)]/2 , \tag{3.5}$$

where we define the constant

$$\Omega_a = \varphi + \omega_a' + \chi_a . \tag{3.6}$$

To characterize the effects of the probe on the interferometer fringes, we define the visibility

$$V \equiv (\langle n_b \rangle_{\max} + \langle n_b \rangle_{\min})^{-1} (\langle n_b \rangle_{\max} - \langle n_b \rangle_{\min})$$
$$= |Z(\chi)| \tag{3.7a}$$

and the phase shift

$$\Delta\varphi \equiv \arg[Z(\chi)] \tag{3.7b}$$

for convenience.

Fringe visibility and fringe displacement are completely determined by $Z(\chi)$. This function depends on the intensity fluctuations in the probe field through the distribution $P_B(n)$ and on the arithmetic of χ. Clearly, for χ an integer multiple of π, $Z(\chi)$ is unity, and the fringe pattern is unaffected by the probe. In general we may think of the sum in Eq. (3.4) as the sum of vectors of length $P_B(n)$ where the angle between each vector is 2χ. [This assumes that there are no "missing" vectors corresponding to values of n such that $P_B(n)=0$.] If χ is a rational multiple of π, a great deal of cancellation may occur in the sum of Eq. (3.4). For example, if $\chi=\pi/2$, the sign of each term alternates, and $Z(\chi)$ is real and possibly much less than unity. This corresponds to a vector of length $P_B(n)$ tending to cancel a vector of length $P_B(n+1)$. Thus, the degree of cancellation depends crucially on the probe field statistics.

Let us assume that the probe field is initially in a coherent state. The single-mode coherent field is generated by a classical current distribution which is closely approximated by a laser. Furthermore, the coherent field is a minimum uncertainty state with respect to the in-phase and out-of-phase quadrature operators given by

$$Y(\phi) = \tfrac{1}{2}(e^{-i\phi} B + e^{i\phi} B^\dagger) \tag{3.8}$$

for $\phi=0$ and $\pi/2$, respectively. Thus, noise introduced by the probe beam is minimized. The coherent state, which is generated from the vacuum by the unitary displacement operator

$$D(\alpha) = \exp(\alpha B^\dagger - \alpha^* B) \tag{3.9}$$

is represented in the number state basis by

$$|\alpha\rangle = D(\alpha)|0\rangle$$
$$= \exp(-|\alpha|^2/2) \sum_n (n!)^{-1/2} \alpha^n |n\rangle , \tag{3.10}$$

and it is straightforward to demonstrate that

$$\exp(i\chi n_B)|\alpha\rangle = |\alpha e^{i\chi}\rangle \tag{3.11}$$

which is a rotation of the original coherent state. Thus, for the probe field initially in the coherent state $|\alpha\rangle$, we obtain the element

$$Z(\chi) = \langle \alpha | \alpha e^{2i\chi} \rangle$$
$$= \exp(-2|\alpha|^2 \sin^2\chi) \exp[i|\alpha|^2 \sin(2\chi)] . \tag{3.12}$$

Therefore, the visibility and phase shift are given by

$$V = \exp(-2|\alpha|^2 \sin^2\chi) \tag{3.13a}$$

and

$$\Delta\varphi = |\alpha|^2 \sin(2\chi) , \tag{3.13b}$$

respectively. The damping of the fringes depends on the strength of the term $|\alpha|^2 \sin^2\chi$. As expected the minimum fringe visibility occurs for $\chi=\pi/2$. It is interesting that at this point the fringe displacement is actually zero.

An increase in the intensity of the probe beam, for fixed nonlinearity χ, leads to an exponential damping of the interference fringes. Furthermore, an increase in the probe field intensity results in an increased phase shift of the field a_2. The damping of the fringes can be interpreted as being due to the intensity fluctuations in the probe field. To show this we consider the fringe visibility for two probe fields, one which has large intensity fluctuations and the other which has no intensity fluctuations. Let us observe the effect of a probe beam which is in the thermal state, a state which exhibits large intensity fluctuations at high temperature.

The mean number of photons in a single-mode thermal state at temperature T is given by the quantity[7]

$$n_T = [\exp(\hbar\omega_B / kT) - 1]^{-1} . \tag{3.14}$$

The photon number probability distribution is given by

$$P(n) = (1+n_T)^{-1} [n_T/(1+n_T)]^n . \tag{3.15}$$

Therefore, the visibility and phase shift are given by

$$V = [1 + 4n_T(1+n_T)\sin^2\chi]^{-1/2} \tag{3.16a}$$

and

$$\tan(\Delta\varphi) = (1 + 2n_T \sin^2\chi)^{-1} n_T \sin(2\chi) . \tag{3.16b}$$

The existence of fringe damping for values of χ which are not integer multiples of π is evident. A phase shift is also induced. For the case of zero temperature, the vacuum result is recovered; the fringes are neither damped nor phase shifted. We further note that, as with the coherent probe, the minimum fringe visibility occurs at $\chi=\pi/2$ for which the fringe displacement is zero.

Alternatively, the intensity fluctuations of the number state are zero. If the probe is in the pure number state $|m\rangle$, then

$$V = 1 \text{ and } \Delta\varphi = 2m\chi . \tag{3.17}$$

The nonzero intensity of the number state for $m>0$ induces a phase change in the a_2 field, but the fringe visibility is not reduced. The visibility is not reduced because

of the absence of fluctuations in photon number for the pure number state, which includes the vacuum state as a special case.

The example with which we are concerned is the case that the probe beam is prepared in a squeezed state. Whereas the coherent state is a minimum uncertainty state with respect to the in-phase and out-of-phase quadratures and the quantum noise is phase independent, the squeezed state is a minimum uncertainty state with reduced fluctuations in one quadrature. As the squeezed state is a minimum uncertainty with respect to the quadrature operators it satisfies the eigenvalue equality[8]

$$(B\cosh r + B^{\dagger}e^{i\theta}\sinh r)|\alpha,\eta\rangle = (\alpha\cosh r + e^{i\theta}\alpha^{*}\sinh r)|\alpha,\eta\rangle \quad (3.18)$$

for

$$r=|\eta| \text{ and } e^{i\theta}=\eta/|\eta| \ . \quad (3.19)$$

The squeezed state is generated from the vacuum by the transformation

$$|\alpha,\eta\rangle = D(\alpha)S(\eta)|0\rangle \ , \quad (3.20)$$

where $D(\alpha)$ is the displacement operator (3.9) and $S(\eta)$ is the unitary squeeze operator[9]

$$S(\eta)=\exp(\tfrac{1}{2}\eta^{*}B^{2}-\tfrac{1}{2}\eta B^{\dagger 2}) \ . \quad (3.21)$$

The squeeze transformation of the annihilation operator is

$$S^{\dagger}BS = B\cosh r - B^{\dagger}e^{i\theta}\sinh r \ . \quad (3.22)$$

The coherent state corresponds to $r=0$, and the squeezed vacuum corresponds to $\alpha=0$. We shall restrict our attention to the case that

$$e^{i\theta/2}=\alpha/|\alpha| \ ; \quad (3.23)$$

hence,

$$\langle\alpha,\eta|B|\alpha,\eta\rangle=\alpha \quad (3.24)$$

and, for $\Delta Y\equiv\langle(Y-\langle Y\rangle)^{2}\rangle^{1/2}$

$$e^{r}\Delta Y(\tfrac{1}{2}\theta)=\tfrac{1}{2}=e^{-r}\Delta Y\left(\frac{1}{2}\theta+\frac{\pi}{2}\right) \ . \quad (3.25)$$

The phase-space representation of the squeezed state mean and dispersion contour are shown in Fig. 2 for r positive which corresponds to reduced intensity fluctuations. The phase fluctuations are reduced for r negative.

The operator $\exp(2i\chi n_B)$ effects a rotation of the squeezed state

$$\exp(2i\chi n_B)|\alpha,\eta\rangle=|\alpha e^{2i\chi},\eta e^{4i\chi}\rangle \ ; \quad (3.26)$$

therefore, $Z(\chi)$ is given by (3.4)

$$Z(\chi)=\langle\alpha,\eta|\alpha e^{2i\chi},\eta e^{4i\chi}\rangle \ , \quad (3.27)$$

the overlap of the squeezed states $|\alpha,\eta\rangle$ and $|\alpha e^{2i\chi},\eta e^{4i\chi}\rangle$. The visibility is, therefore,

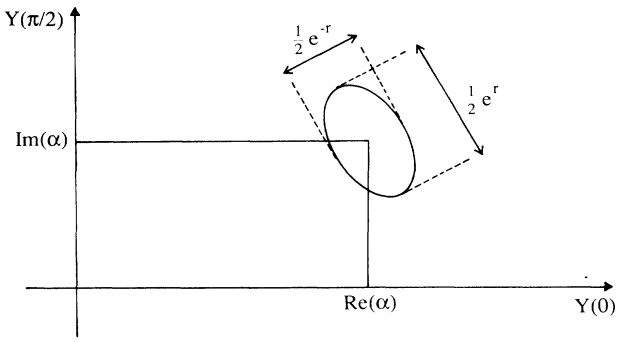

FIG. 2. The phase-space plot of the squeezed state $|\alpha,\eta\rangle$ with squeezed intensity fluctuations ($r>0$). $Y(0)$ is the in-phase quadrature and $Y(\pi/2)$ is the out-of-phase quadrature.

$$V=\kappa^{1/2}\exp(-e^{2r}|\alpha|^{2}\{1-\kappa\cos(2\chi+\delta)+\tfrac{1}{2}\kappa[\cos(4\chi+\delta)-\cos\delta]\sinh(2r)\}) \quad (3.28a)$$

and the phase shift is

$$\Delta\varphi=\tfrac{1}{2}\delta+\kappa e^{-2r}|\alpha|^{2}\{\sin(2\chi+\delta)-\tfrac{1}{2}[\sin(4\chi+\delta)-\sin\delta]\sinh(2r)\} \ . \quad (3.28b)$$

The visibility coefficient

$$\kappa=[1+\sinh^{2}(2r)\sin^{2}(2\chi)]^{-1/2} \quad (3.29)$$

and the phase

$$\delta=\tan^{-1}\left[\frac{\tanh^{2}r\sin 4\chi}{1-\tanh^{2}r\cos 4\chi}\right] \quad (3.30)$$

depend on the degree of squeezing and the nonlinearity. If the probe field is not squeezed or the nonlinearity is zero, $\kappa=1$ and $\delta=0$.

For the squeezed vacuum, $V=\kappa^{1/2}$. A plot of visibility versus χ/π is shown in Fig. 3. Whereas the vacuum produces perfect visibility for all values of χ, the visibility for the squeezed vacuum is less than unity except for when χ is an integer multiple of $\pi/2$. The visibility is unity for $\chi=\pi/2$ because the squeezed vacuum contains only even photons,[9] and every odd term in (3.4) is zero. Maximum partial cancellation occurs for $\chi=\pi/4$, $3\pi/4$ for the squeezed vacuum in (3.4). In Fig. 3 the visibility is seen to be at a minimum for these values of χ.

Let us consider the visibility for a general squeezed state. In the limit of weak squeezing, for example, $\kappa\rightarrow 1$ and $\delta\rightarrow 0$. The visibility is approximated by

$$V\cong\exp\{-2|\alpha|^{2}\sin^{2}\chi[1-2r\cos(2\chi)]\} \ . \quad (3.31)$$

The visibility is a small modification of that for the coherent field (3.13a). Positive squeezing ($r>0$) results in improved visibility for $0\le\chi<\pi/4$, but negative squeezing ($r>0$) improves the visibility for $\pi/4<\chi\le\pi/2$ due to the dependence of the visibility on the overlap.

In Figs. 4(a) and 4(b) the visibility versus χ is presented

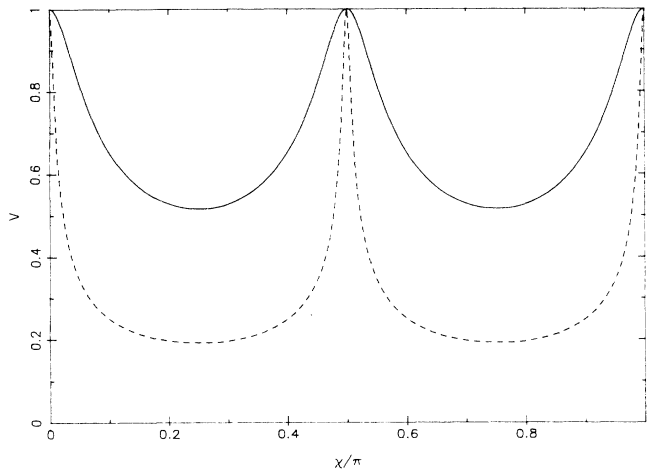

FIG. 3. Fringe visibility V vs the nonlinearity χ for the squeezed vacuum, where $r=\pm 1$ (solid line) and $r=\pm 2$ (dash line). For the unsqueezed vacuum ($r=0$), $V=1$ for all χ.

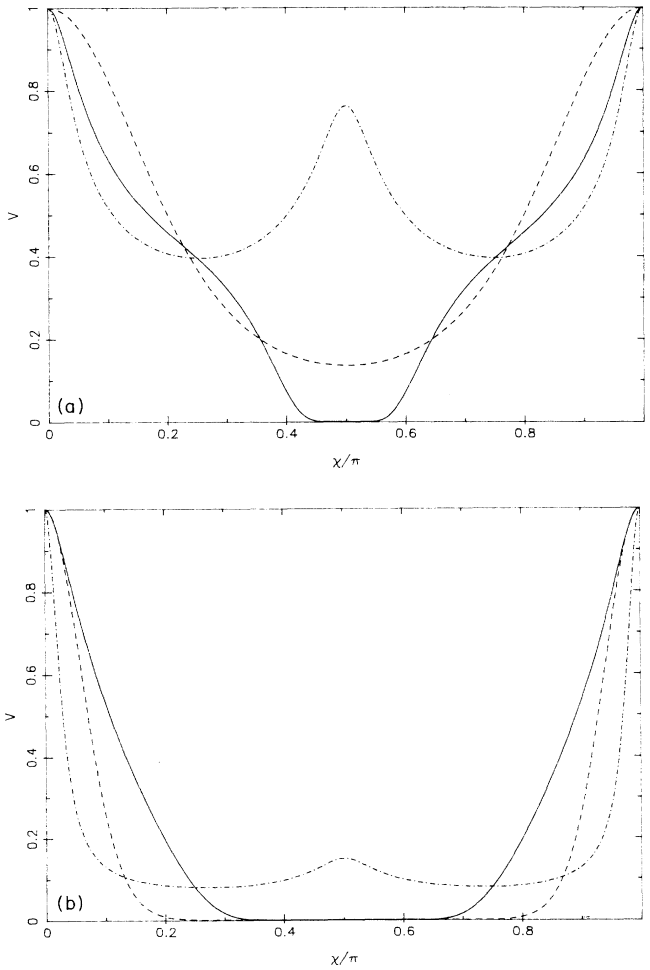

FIG. 4. Fringe visibility V vs the nonlinearity χ/π for the squeezed state $|\alpha,\eta\rangle$, where (a) $|\alpha|^2=1$, (b) $|\alpha|^2=7$ and $|\eta|=1$ (solid line), $|\eta|=0$ (dash line), and $|\eta|=-1$ (dash-dot line).

for the coherent field and for moderately squeezed fields. The graphs are periodic over π and symmetric about $\pi/2$. For low $|\alpha|^2$ [Fig. 4(a)] and low χ the visibility is better for the coherent field than for either moderately squeezed field ($r=\pm 1$) although we have seen for weak squeezing that a small positive value for r will result in better visibility than for $r=0$. For $|\alpha|^2$ moderate [Fig. 4(b)] and χ small, positive squeezing ($r>0$) results in improved visibility. For $\chi=\pi/2$ the visibility is improved for negative squeezing which attains a local maximum at $\chi=\pi/2$. The visibility for the squeezed states at $\chi=\pi/2$ is given by

$$V_{\chi=\pi/2}=\exp(-2e^{2r}|\alpha|^2)\ . \tag{3.32}$$

The exponential decay of visibility as $|\alpha|^2$ increases can be greatly reduced for $\chi=\pi/2$ by using a strongly squeezed ($r<0$) probe field.

IV. PROBE QUADRATURE PHASE MEASUREMENT AND PHOTON PATH INFERENCE

The probe field interacts with the field in arm 2 of the interferometer via the nonlinear Kerr medium. The field in arm 2 is hereafter referred to as the signal field. The presence of a photon in the signal field produces a phase shift in the probe; the phase does not change if there is no photon in the signal field. The phase shift is measured by the quadrature phase measurement apparatus whose location is shown in Fig. 1. The operator associated with the measurement is the quadrature phase operator [cf. (3.8)]

$$Y(\phi)=\tfrac{1}{2}(e^{-i\phi}B'+e^{i\phi}B'^{\dagger})\ , \tag{4.1}$$

where ϕ is the reference phase of the apparatus and B' is the postinteraction probe field annihilation operator (2.5b). The single-model quadrature phase measurement, which we are assuming here, is closely approximated by a balanced homodyne detector.[10]

The probe field itself undergoes an intensity-dependent phase shift in passing through the Kerr medium. Phase fluctuations in the probe which are induced by the probe intensity fluctuations due to the nonlinear self-coupling is observed in studies of the nonlinear oscillator.[11,12] It is convenient to remove the intensity-dependent phase shift prior to the quadrature phase measurement. To do this we pass the probe field through a further length of nonlinear Kerr medium outside the interferometer. The length is adjusted so that the total self-induced phase shift is an integer multiple of 2π. When this is done, χ_B is effectively zero and

$$B'=B\exp(-2i\chi n_2)\ . \tag{4.2}$$

The distribution of quadrature phase readings is given by

$$P(y)=\mathrm{tr}[\,|y\rangle_B\langle y|\exp(-2i\chi n_2 n_B)\times\rho(0)\exp(2i\chi n_2 n_B)]\ , \tag{4.3}$$

where $|y\rangle_B$ is an eigenstate of $Y(\phi)$ and $\rho(0)$ is the preinteraction density matrix

$$\rho(0)=|\Psi\rangle\langle\Psi|\otimes\rho_B \tag{4.4}$$

for $|\Psi\rangle$ the interferometer state (3.3) and ρ_B the probe field density operator. Performing the partial trace over the field in arm 1 of the interferometer, we have

$$P(y)=\mathrm{tr}_{2,B}[\,|y\rangle_B\langle y|\exp(-2i\chi n_2 n_B)\times\rho'(0)\exp(2i\chi n_2 n_B)]\ , \tag{4.5}$$

where

$$\rho'(0)=\tfrac{1}{2}(|0\rangle_2\langle 0|+|1\rangle_2\langle 1|)\otimes\rho_B\ , \tag{4.6}$$

i.e., the field in arm 2 of the interferometer is a mixed state of zero and one photon. In Sec. III we consider examples of ρ_B, including the vacuum, the thermal state, the number state, and the coherent and squeezed states. Performing the partial trace over the signal field, the distribution of readings of y

$$P(y)=\tfrac{1}{2}P_0(y)+\tfrac{1}{2}P_1(y) \tag{4.7}$$

is obtained, where

$$P_0(y)=\mathrm{tr}(|y\rangle_B\langle y|\rho_B) \tag{4.8}$$

is the probability distribution for measuring no photon in the signal field and

$$P_1(y)=\mathrm{tr}[|y\rangle_B\langle y|\exp(-2i\chi n_B)\rho_B\exp(2i\chi n_B)] \tag{4.9}$$

is the distribution of readings if the signal field consists of one photon.

Each measurement of y is used to decide whether a photon has been observed. The decision is equivalent to inferring the path of the photon. The quality of the inference is as good as the accuracy of deciding to which distribution y belongs. As the accuracy increases and we become more certain of the path, the corpuscular behavior of the photon is becoming more evident. The accuracy improves as the overlap between the distributions is reduced. The zero-amplitude states do not allow for an inference; consequently, the thermal state and the number state will not be considered as probe field states. The probe field states are restricted to the quadrature phase minimum uncertainty states: the coherent and squeezed states.

The normalized quadrature phase reading

$$c\equiv|\langle B\rangle|^{-1}y \tag{4.10}$$

is introduced for $\langle B\rangle=\mathrm{tr}(\rho_B B)\neq 0$. The quadrature phase signal we are interested in is the difference between the readings for a photon being present and absent in the signal field. The mean signal is $\langle c_0\rangle-\langle c_1\rangle$ where the nth moment of the distribution is

$$\langle c_{0,1}^n\rangle=\int dc\, c^n P_{0,1}(c) \tag{4.11}$$

with $P_{0,1}(c)$ obtained from Eqs. (4.8) and (4.9) by the change of variable (4.10), and the noise for each distribution is given by

$$\Delta c_{0,1}=\langle(c_{0,1}-\langle c_{0,1}\rangle)^2\rangle^{1/2}\ . \tag{4.12}$$

The signal-to-noise ratio (SNR) for the normalized quadrature phase measurement is

$$\sigma=\frac{|\langle c_0\rangle-\langle c_1\rangle|}{(\Delta c_0^2+\Delta c_1^2)^{1/2}}\ . \tag{4.13}$$

Good inferences are obtained if $\sigma\gtrsim 2$, and the inference is poor if $\sigma\lesssim 1$. The SNR is improved by increasing the separation of the distribution means and reducing the widths.

The probe field is in a squeezed state with the density operator

$$\rho_B=|\alpha,\eta\rangle\langle\alpha,\eta|\ . \tag{4.14}$$

The phase of the squeezed state relative to the quadrature phase measurement reference phase is chosen such that α and $\eta=r$ are real. Using the quadrature phase eigenstate representation for squeezed states,[10] we obtain

$$P_0(y)=(\tfrac{1}{2}\pi e^{-2r})^{-1/2}\exp[-2e^{2r}(y-\alpha)^2]\ . \tag{4.15}$$

For the case that a photon is detected in the signal field, we apply (3.26) to (4.14) to obtain

$$P_1(y)=[\tfrac{1}{2}\pi(e^{-2r}\cos^2 2\chi+e^{2r}\sin^2 2\chi)]^{-1/2}\times\exp[-2(e^{-2r}\cos^2 2\chi+e^{2r}\sin^2 2\chi)^{-1}\times(y-\alpha\cos 2\chi)^2]\ . \tag{4.16}$$

Using the expectation value

$$\langle\alpha,\eta|B|\alpha,\eta\rangle=\alpha\ , \tag{4.17}$$

the substitution of (4.10) into (4.15) and (4.16) produces the distribution

$$P_0(c)=\alpha(\tfrac{1}{2}\pi e^{-2r})^{-1/2}\exp[-2\alpha^2 e^{2r}(c-1)^2] \tag{4.18}$$

and

$$P_1(c)=\alpha[\tfrac{1}{2}\pi(e^{-2r}\cos^2 2\chi+e^{2r}\sin^2 2\chi)]^{-1/2}\times\exp[-2\alpha^2(e^{-2r}\cos^2 2\chi+e^{2r}\sin^2 2\chi)^{-1}\times(c-\cos 2\chi)^2]\ , \tag{4.19}$$

respectively. The mean normalized quadrature phase signal is

$$\langle c_0\rangle-\langle c_1\rangle=1-\cos 2\chi=2\sin^2\chi \tag{4.20}$$

and the SNR (4.13) is

$$\sigma=4\alpha[e^{-2r}(1+\cos^2 2\chi)+e^{2r}\sin^2 2\chi]^{-1/2}\sin^2\chi\ . \tag{4.21}$$

The SNR is improved by increasing α and has a maximum for $\chi=\pi/2$. In this case

$$\sigma_{\chi=\pi/2}=2^{3/2}e^r\alpha\ , \tag{4.22}$$

and the SNR is improved by using a positively squeezed probe field ($r>0$). The SNR is also improved by increasing α.

In Fig. 5 the normalized SNR, σ/α, versus χ/π is presented. The positively squeezed field provides a superior SNR for $\chi\cong\pi/2$ [whereas a negatively squeezed field improves visibility in expression (3.32)]. However, for χ small, negative squeezing produces a better SNR and for

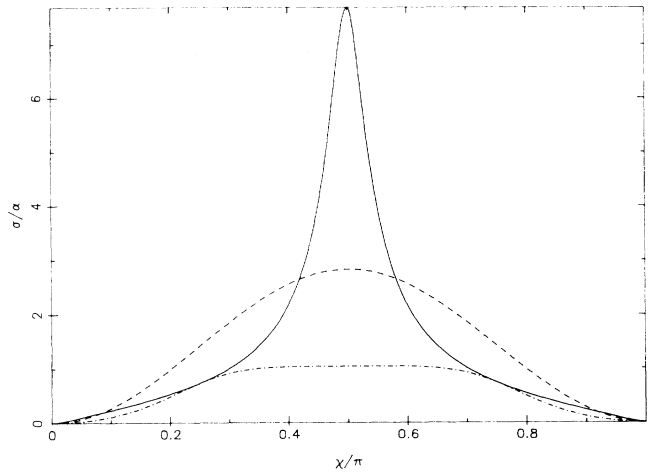

FIG. 5. Normalized signal-to-noise ratio σ/α vs χ/π for the squeezed state $|\alpha,\eta\rangle$, where α and $\eta=r$ are real, and $r=1$ (solid line), $r=0$ (dash line), and $r=-1$ (dash-dot line).

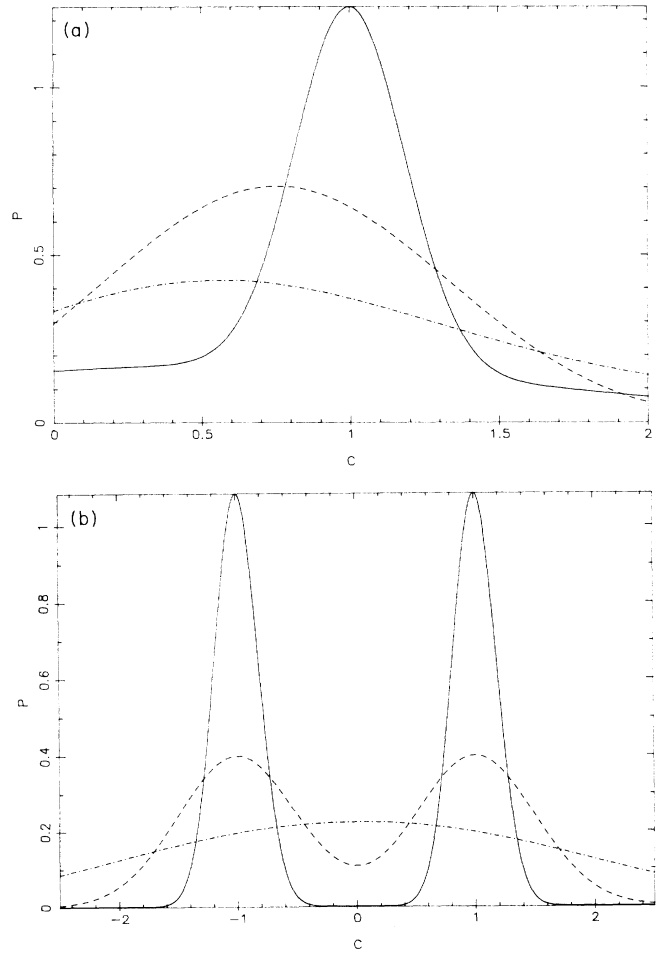

FIG. 6. The probability distribution P vs the normalized probe field quadrature phase readings c for the squeezed state $|\alpha,\eta\rangle$, where $\alpha=1$ and $\eta=r$ are real. The nonlinearity assumes the values (a) $\chi=\pi/6$ and (b) $\chi=\pi/2$. The squeezing parameters are $r=1$ (solid line), $r=0$ (dash line), and $r=-1$ (dash-dot line).

$\chi=\pi/4$, the coherent field produces the best SNR. The sign of the squeezing parameter r which produces the best SNR depends on whether $\chi<\pi/4$ or $\chi>\pi/4$. For small values of χ, however, the normalized SNR is much less than one. Increasing α increases σ proportionally, though, and a good inference of the photon path can be made for small χ if the probe field is sufficiently strong.

The probability distribution $P(c)$ is presented in Fig. 6(a) for $\chi=\pi/6$ and $\alpha=1$ and in Fig. 6(b) for $\chi=\pi/2$ and $\alpha=1$. For $\chi=\pi/6$ [Fig. 6(a)] the two distributions $P_0(c)$ and $P_1(c)$ are difficult to distinguish. Indeed for these values Fig. 5 confirms that $\sigma<1$ in each case, and the inference is poor, as expected. However, as the probe intensity increases, the SNR increases proportional to α; the distributions $P_0(c)$ and $P_1(c)$ eventually become distinguishable as α increases. The distributions are distinguishable for $\chi=\pi/2$, $\alpha=1$, and r non-negative [Fig. 6(b)]. This is not surprising as $\sigma>1$ for r nonnegative, but $\sigma<1$ for $r=-1$ (see Fig. 5). An increase in the probe strength will lead to better inferences of the photon path. The quantity σ is an accurate measure of the quality of the inference for a probe field which is a coherent or squeezed state.

V. COMPLEMENTARITY

The fringe visibility quantifies the wavelike behavior of the photon; the SNR quantifies the corpuscular behavior. The two quantities are, therefore, complementary. We compare the visibility to the SNR for various parameter values to consider how to optimize the observations of complementary quantities.

In Fig. 7(a) the visibility versus SNR is plotted for the coherent state corresponding to various values of χ. In each case an increase in the SNR corresponds to a decrease in the visibility as we expect. That is, an increase in the certainty of the photon path reduces the fringe visibility which exhibits the wavelike nature. By combining the expressions (3.13a) and the SNR for a coherent probe field [cf. (4.19) for $r=0$)

$$\sigma=2^{3/2}\alpha\sin^2\chi\ , \tag{5.1}$$

we obtain the relation between the visibility and the SNR

$$V=\exp\left[-\frac{1}{4}\frac{\sigma^2}{\sin^2\chi}\right]\ . \tag{5.2}$$

The visibility versus SNR graphs in Fig. 7(a) satisfy (5.2), and it is clear from (5.2) that the optimal visibility versus SNR relation is obtained for $\chi=\pi/2$.

In Fig. 7(b) the visibility versus SNR graphs are computed for the squeezed state $r=1$. Again the optimal relation is obtained for $\chi=\pi/2$. By combining the expression for visibility (3.32) and the SNR (4.20) for $\chi=\pi/2$, we observe that

$$V_{\chi=\pi/2}=\exp(-\tfrac{1}{4}\sigma^2) \tag{5.3}$$

is true, and the curve is independent of whether the probe

field is squeezed. However, using a squeezed state can improve either the visibility or the SNR. For other values of χ, squeezing the field can improve the visibility for large values of SNR, as shown in Fig. 8 for $\chi=\pi/6$, but the optimal relation (5.3) represents the limit for observing the complementary quantities visibility and SNR for a squeezed-state probe field.

The experimental implementation of the scheme discussed in this paper must be regarded as being at the limits of current technology. The available Kerr nonlinearities are simply too small. A high but realistic value for a third-order nonlinearity $\chi^{(3)}$ is approximately 10^{-5} esu (Ref. 13) which, in SI units, is approximately 10^{-23}.[14] The χ used in this paper is related to $\chi^{(3)}$ by[15]

$$\chi\cong\chi^{(3)}\left[\frac{\hbar\omega^2}{2\epsilon_0^2 V}\right]\frac{L}{c}\ , \tag{5.4}$$

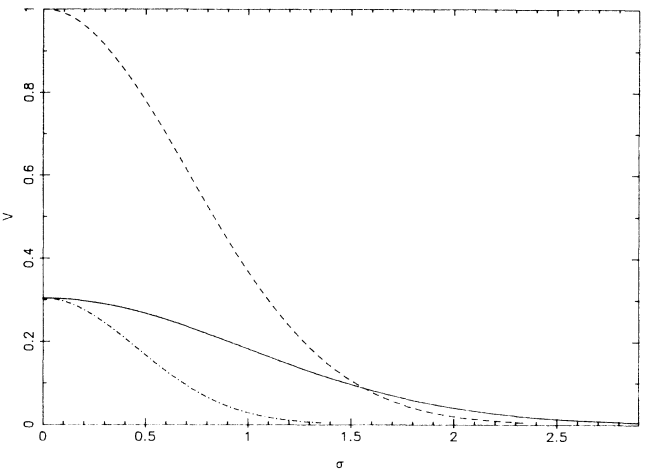

FIG. 8. The visibility V vs the SNR σ for $\chi=\pi/6$, and the squeeze parameter is $r=1$ (solid line), $r=0$ (dash line), and $r=-1$ (dash-dot line).

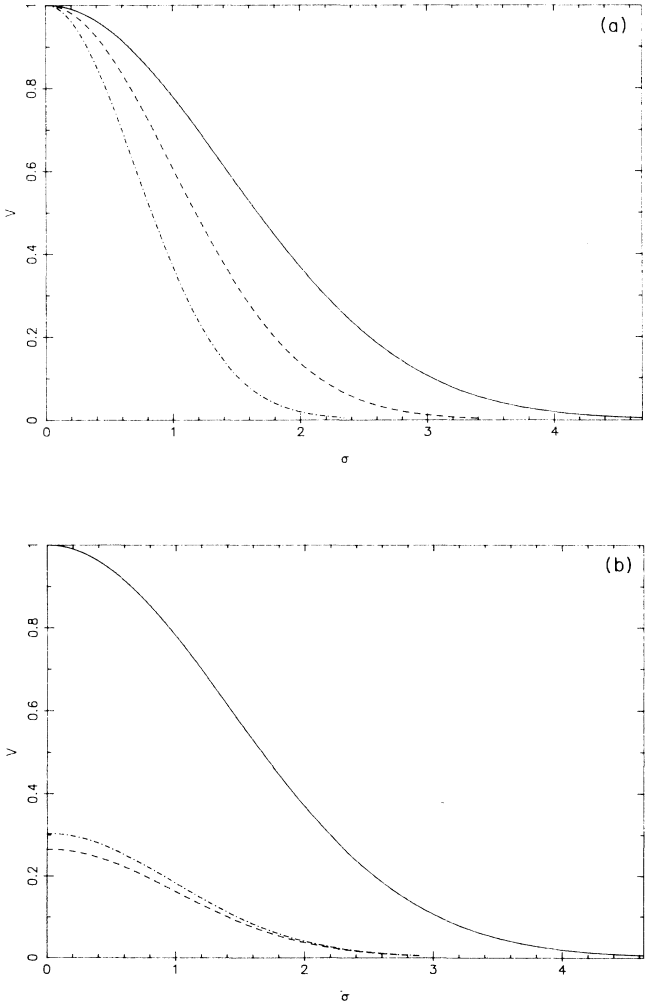

FIG. 7. The visibility V vs the SNR σ for (a) the coherent state and (b) the squeezed state ($r=1$) for $\chi=\pi/2$ (solid line), $\chi=\pi/4$ (dash line), and $\chi=\pi/6$ (dash-dot line).

where V is the interaction volume, L is the length of the nonlinear medium, and c the speed of light.

At $\omega\simeq 5\times 10^{14}$ Hz this gives $\chi\cong 10^{-6}$ rad for a 1-m length. The phase shift induced by a single photon in the signal field would be difficult to detect but not impossible. Recently Xiao *et al.*[16] employed a squeezed-state technique to measure a phase change near this limit. The small value of χ produces a visibility-SNR relation which is far from the optimal case. For small χ and a coherent probe field the visibility is approximated by (3.13a)

$$V\cong\exp(-2\alpha^2\chi^2) \tag{5.5}$$

and

$$\sigma\cong 2^{3/2}\alpha\chi^2\ . \tag{5.6}$$

For $\chi\cong 10^{-6}$, the visibility decays to zero as the probe intensity rises to 10^{12} photons, but 10^{24} photons in the probe field are necessary for a good SNR. The fringes fade long before good values of SNR are obtained for small χ. Nevertheless the corpuscular and wavelike properties of the photon are observed in the same apparatus, and the observed behavior depends on the continuous probe field intensity parameter. Furthermore, despite the difficulty of realizing the scheme described here, it nonetheless provides a clean illustration of how complementarity is enforced in a QND experiment and is rather more realistic than similar discussions of complementarity based on the two-slit experiment.

ACKNOWLEDGMENTS

We would like to thank Dr. S. Braunstein for useful discussions. This work has been supported by the Australian Research Council.

[1]P. Grangier, G. Roger, and A. Aspect, Europhys. Lett. **1**, 173 (1986).
[2]G. J. Milburn and D. F. Walls, Phys. Rev. A **28**, 2065 (1983).
[3]N. Imoto, H. A. Haus, and Y. Yamamoto, Phys. Rev. A **32**, 2287 (1985).
[4]O. R. Frisch, Contemp. Phys. **7**, 45 (1965) [reprinted in *Concepts of Quantum Optics*, edited by P. L. Knight and L. Allen (Pergamon, Oxford, 1983), p. 105].
[5]P. Alsing, G. J. Milburn, and D. F. Walls, Phys. Rev. A **37**, 2970 (1988).
[6]H. A. Bachor, M. D. Levenson, D. F. Walls, S. H. Perlmutter, and R. M. Shelby, Phys. Rev. A **38**, 180 (1988).
[7]R. Loudon, *The Quantum Theory of Light*, 2nd. ed. (Oxford University Press, Oxford, 1983).
[8]H. P. Yuen, Phys. Rev. A **13**, 2226 (1976).
[9]R. Loudon and P. L. Knight, J. Mod. Opt. **34**, 709 (1987).
[10]H. P. Yuen and J. H. Shapiro, in *Coherence and Quantum Optics IV*, edited by L. Mandel and E. Wolf (Plenum, New York, 1980), p. 719.
[11]G. J. Milburn, Phys. Rev. A **33**, 674 (1986).
[12]M. Kitigawa and Y. Yamamoto, Phys. Rev. A **34**, 3974 (1986).
[13]R. E. Slusher, S. L. McCall, A. Mysyrowicz, and S. Schmitt-Rink, in *XVI International Conference on Quantum Electronics Technical Digest* (The Japan Society of Applied Physics, 1988), pp. 472–473.
[14]D. M. Pepper and A. Yariv, in *Optical Phase Conjugation*, edited by R. A. Fisher (Academic, New York, 1983), p. 24.
[15]P. D. Drummond and D. F. Walls, J. Phys. A **13**, 725 (1980).
[16]M. Xiao, L.-A. Wu, and H. J. Kimble, Phys. Rev. Lett. **5**, 278 (1987).